

## TEST PROGRAM FOR THE ZEUS CALORIMETER

Robert KLANNER

DESY, Notkestrasse 85, D-2000 Hamburg 52 FRG

This talk covers some of the experimental studies which have led to the design of the ZEUS uranium scintillator calorimeter. It is shown how, by varying the scintillator to uranium ratio, equal response for electrons and hadrons and optimum hadronic energy resolution ( $\sigma_E/E \sim 35\%/\sqrt{E}$ ) over a wide energy range can be achieved. A similar optimisation has been done for a lead scintillator calorimeter, and almost equal response for hadrons and electrons together with a hadronic energy resolution of  $\sim 44\%/\sqrt{E}$  up to  $\sim 75$  GeV has been achieved. Various practical aspects of calorimetry using scintillator as detector material will also be discussed. The work described in this talk has been done by many members of the ZEUS collaboration.

### 1. Introduction

The electron collider HERA, presently under construction at DESY, Hamburg, will collide 30 GeV electrons with 820 GeV protons in 1990. Two multipurpose detectors, H1 and ZEUS, are in preparation to exploit the physics of HERA.

Fig. 1 shows a schematic view of the ZEUS detector [1]. The topic of this paper is the ZEUS high resolution calorimeter CAL, which attempts to achieve the following performance:

- (i) hermeticity for energy measurement over the entire solid angle, excluding only a small region around the beam pipe,
- (ii) best achievable energy resolution for hadrons and hadron jets independent of the jet fragmentation,
- (iii) absolute calibration of the energy scale as well as long term stability and uniformity of the energy scale to better than 2%,
- (iv) angular resolution for jets of  $\sim 10$  mrad,
- (v) energy resolution for electrons of about  $\sim 15\%/\sqrt{E[\text{GeV}]}$  and good electron hadron separation,
- (vi) signals shorter than the HERA bunch crossing time of 96 ns.

The technical solution chosen by the ZEUS collaboration is a sampling calorimeter using plates of depleted uranium as absorber and plastic scintillator, read out via plastic wavelength shifter bars, as detector. This talk describes the main features of the proposed calorimeter and the present status of its design.

The sampling structure has been chosen after detailed experimental and theoretical studies of the response of calorimeters with different uranium and scintillator thicknesses to hadrons, electrons and muons for energies between 3 and  $\sim 100$  GeV. These measurements confirm the recent calculations by Brückmann et al. [2] and Wigmans [3]. They show how the proper detection of the slow neutron component of hadronic showers can be used to optimize the response of hadronic calorimeters. As an extension of this work, a lead scintillator calorimeter has been built, which confirms the prediction that equal average response for electrons and hadrons, and good hadron resolution can also be achieved for absorbers other than depleted uranium.

The second part of the talk discussed more practical aspects of calorimetry using scintillator as readout material, in particular the question of non-uniformity of response at the boundary between calorimeter modules

Table 1  
Parameters of the ZEUS high resolution calorimeter

Name	FCAL	BCAL	RCAL
Range in polar angle	2.2°–36.7°	36.7°–129.1°	129.1°–176.5°
Depth in interaction length	7 $\lambda$	5 $\lambda$	4 $\lambda$
No. of long. readout segments	3	3	2
No. of readout channels	4264	5184	3392
Total absorber weight	171 t	230 t	98 t
Total scintillator weight	8 t	10 t	5 t

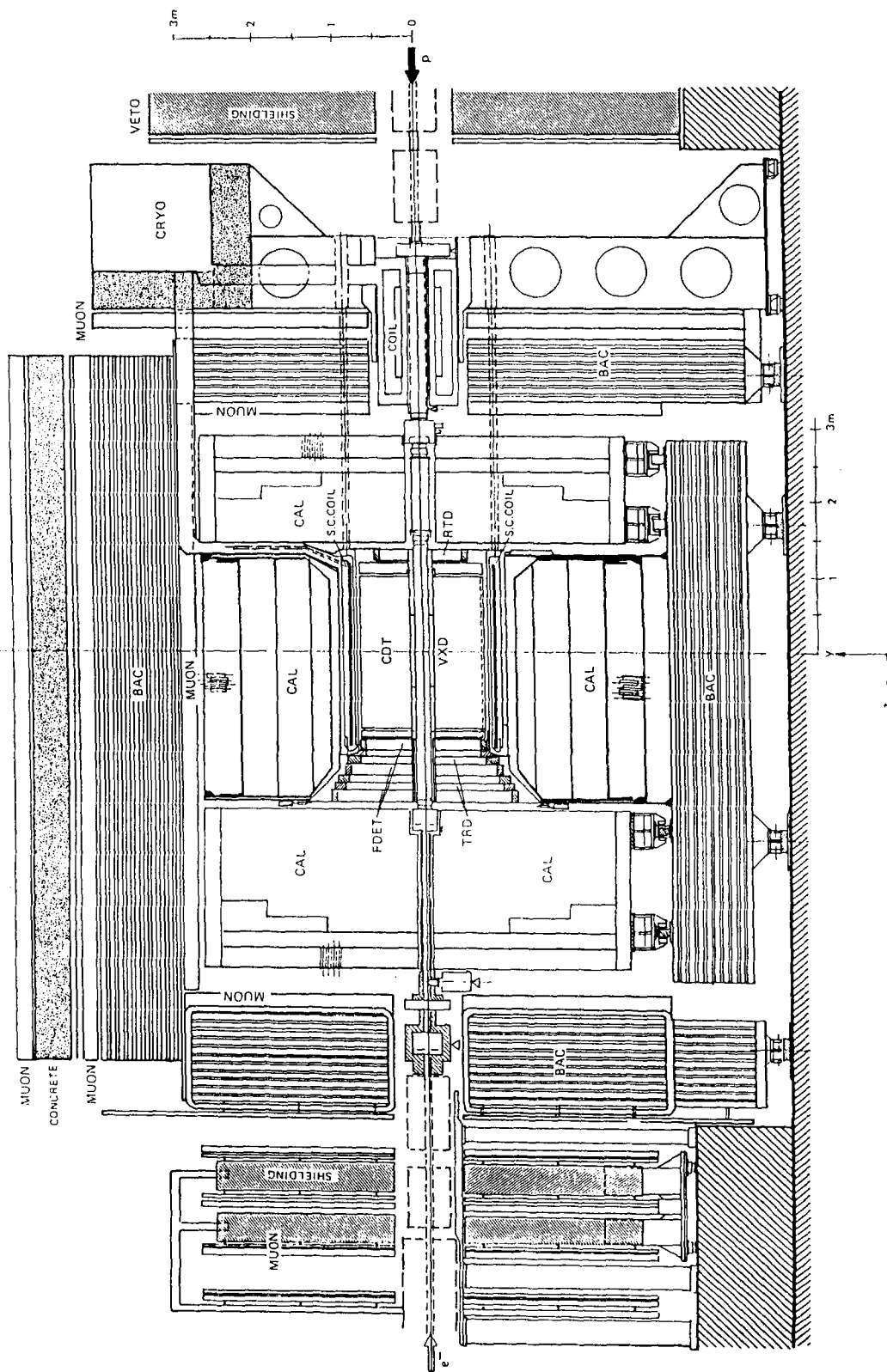


Fig. 1. Layout of the ZEUS detector - cut along the beam.

due to wavelength shifters, and finally the sensitivity to radiation damage of plastic scintillator and wavelength shifter bars.

## 2. Layout and design of the ZEUS calorimeter

The layout of the ZEUS detector (fig. 1) shows that the high resolution calorimeter "CAL" consists of the forward (FCAL), the barrel (BCAL) and the rear section (RCAL). Table 1 gives information on the angular coverage, the depth of the different sections, and number of readout channels.

The BCAL consists of 32 identical segments forming a barrel concentric around the HERA beams. FCAL and RCAL consists of rectangular boxes which build up two walls perpendicular to the beam pipe. The sampling structures in all sections and along the entire depth of the calorimeter are identical: 3.3 mm thick plates of depleted uranium "DU" with  $\sim 1.7\%$  Nb (density  $\sim 18.5$  g/cm<sup>3</sup>), clad in stainless steel (0.2 mm for the first 25 plates and 0.4 mm for the remainder) alternate with 2.6 mm thick sheets of plastic scintillator "SCI" (SCSN-38 from Kyowa). The longitudinal and transverse segmentations are achieved by wavelength shifter bars "WLS". All scintillator tiles are read out from two sides for good uniformity and additional spatial information through "light-division".

The first 25 DU-plates constitute the electromagnetic sections. They are read out by scintillator tiles of about  $5 \times 20$  cm area. In the BCAL, whose electromagnetic section is projective in both  $\theta$  and  $\phi$ , the dimensions of the scintillators increase with depth. FCAL and RCAL are nonprojective. The electromagnetic section is followed by the hadronic sections: one in the RCAL and two in the BCAL and in the FCAL, with depths as given in table 1. The transverse segmentation is  $20 \times 20$  cm for FCAL and RCAL. These sections of the BCAL are projective in  $\phi$  but nonprojective in  $\theta$ ; the dimension of the scintillator tiles is  $20 \times 20$  cm, when projected onto the front face of the calorimeter. This segmentation results in a total of 7612 photomultipliers for the electromagnetic sections and 5228 for the hadronic sections for all of the calorimeter sections.

Fig. 2 shows a simplified drawing of one of the modules of the FCAL. The module has a sensitive area of  $20 \times 460$  cm (width  $\times$  height). The mechanical elements are a C-frame, the DU-plates, an Al front plate and spacers separating the plates. The DU-plates are connected via profiles to the upper and the lower legs of the C-frame. Highly tensioned steel straps connect the front plate to the back beam thus clamping the DU-plates. They apply enough force through the spacers so that the module can resist accelerations during transport and installation. The figure also shows the scintillator tiles as well as the wavelength shifter plates and light

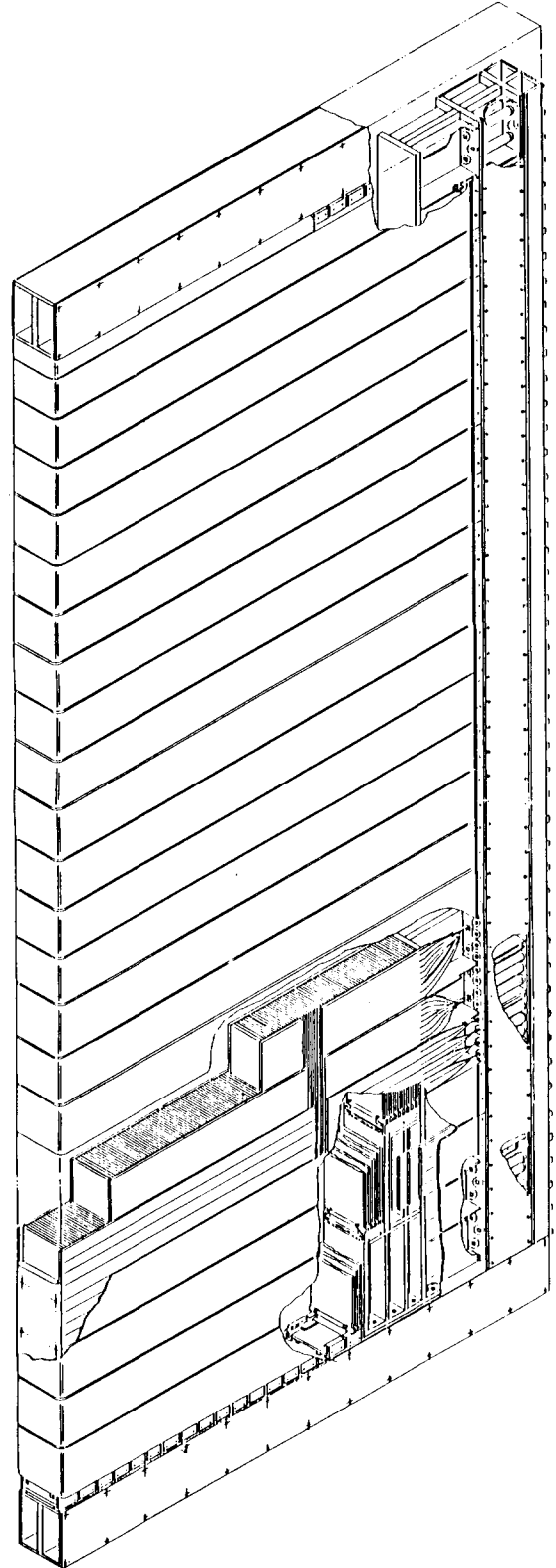


Fig. 2. Layout of a ZEUS FCAL module.

guides which transport the light to the photomultipliers located at the back of the modules. The gap between the edges of the uranium plates of adjacent modules, which contains the wave shifters, mechanical structures and enclosure for gas and light sealing, is 1 cm at the electromagnetic section. It increases to 2 cm at the end of the calorimeter. The design of the BCAL modules is similar, and we refer to [1] for details. The depth of the high resolution calorimeter has been determined from the requirement that, for 90% of the jets with the maximum jet energy expected in any particular region of the calorimeter, the energy containment is 95%. In this way a high resolution sample of events can be selected in the physics analysis with 90% efficiency using the backing calorimeter (BAC in fig. 1) as off-line veto. This optimisation was done using the measured longitudinal shower distributions of hadrons and electrons in a uranium scintillator calorimeter [4] as input into the Lund Monte Carlo code for simulating jets [5].

### 3. Energy resolution and the $e/h$ ratio

This section investigates the following questions for calorimeters using scintillator as detector and depleted uranium or lead as absorber:

- (i) how does the energy resolution depend on the thickness of the materials ( $d_{\text{SCI}}$ ,  $d_{\text{ABS}}$ )?
- (ii) under which conditions can equal response for the hadronic and the electromagnetic component be achieved?

For our study we have been guided by the present understanding of calorimetry [2,3], which we sketch in a simplified way:

–the energy of the incident hadron is deposited in the calorimeter in form of:

- (i) the electromagnetic component ( $\gamma$ ,  $e$ ),
- (ii) ionising charged hadrons ( $\pi$ ,  $p$ , etc.),
- (iii) nuclear binding energy,
- (iv) low energy (20 MeV) neutrons from nuclear evaporation and the low energy tail of the intranuclear cascade; neutrons coming from nuclear

reactions introduced by secondary neutrons are of less importance,

- (v) low energy  $\gamma$ 's from nuclear deexcitation.

–the hadronic energy resolution  $\sigma_h/E_h$  has contributions from sampling fluctuations, which get reduced, if the sampling frequency is increased, and which decrease with increasing energy as  $\sigma_h/E_h \propto 1/\sqrt{E_h}$ .

–additional contributions to  $\sigma_h/E_h$  come from the fluctuations in the way the energy is deposited and the corresponding detection efficiencies. This term decreases slower than  $1/\sqrt{E_h}$  with increasing energy, and therefore frequently dominates the energy resolution at high energies. It is minimal if electrons and hadrons give the same response abbreviated as  $e/h=1$ . In first approximation  $e/h$  depends for a given choice of materials on  $d_{\text{ABS}}/d_{\text{SCI}}$  in the following way:

The response of the contributions (i) and (ii) just depends on the ratio  $d_{\text{SCI}}/d_{\text{ABS}}$ . The term (iii) is not detected at all. The total energy lost in nuclear binding energy however is strongly correlated with the energy given to low energy neutrons (iv). The detection efficiency for the slow neutrons is approximately independent of  $d_{\text{SCI}}$ . Neutrons lose most of their energy by scattering elastically off the free protons of the scintillator, and hardly any via scattering off the heavy uranium nuclei. Since the interaction length of slow neutrons in a typical calorimeter is large compared to the dimensions of the layer structure, decreasing  $d_{\text{SCI}}$  just results in an energy deposition further away from the interaction point where the neutrons have been produced. The energy deposited in the scintillator however is hardly reduced if the calorimeter is of sufficient size. We thus expect that  $e/h$  decreases with increasing  $d_{\text{ABS}}/d_{\text{SCI}}$ . As the neutrons take a finite time until they lose their energy in the scintillator we expect  $e/h$  to decrease with increasing integration time. This has actually been observed experimentally [4].

The contribution (v) is detected only with low efficiency, if scintillator is used as detector, and can be neglected in a qualitative discussion.

Quantitative predictions for  $e/h$  and energy resolutions can be found in [2,3]. For a scintillator thickness

Table 2  
Uranium scintillator test calorimeters

Name	WA 78/HERA	T35	T60A	T60B
$d(\text{DU})$ [mm]	10	3	3.2	3.2
$d(\text{SCI})$ [mm]	5 (Ne 110)	2.5 (SCSN-38)	5 (SCSN-38)	3 (SCSN-38)
Depth [ $\lambda$ ]	5.5 + back	4.2	4.4	6.0 + back
Area [cm <sup>2</sup> ]	60 × 60	60 × 60	60 × 60	60 × 60
Effective $\lambda$ [cm]	19.1	18.2	33.3	25.7
Trans. segmentation [cm]	60 × 60	20 × 20	5 × 60	5 × 60
Long. segmentation [ $\lambda$ ]	0.45	4.2	1.1	1.5
Energy range [GeV]	5–210	3–9	3–9	10–100
Reference	[4]	[6]	[7]	[7]

Table 3  
Lead scintillator test calorimeters

Name	T60C	T36
$d(\text{Pb})$ [mm]	5	10
$d(\text{SCI})$ [mm]	5 (SCSN-38)	2.5 (SCSN-38)
Depth [ $\lambda$ ]	4	5 + back
Area [ $\text{cm}^2$ ]	$60 \times 60$	$68.4 \times 66$
Effective interaction length [cm]	37.1	22.1
Transverse readout segmentation [ $\text{cm}^2$ ]	$5 \times 60$	$22.8 \times 22$
Longitudinal readout segmentation [ $\lambda$ ]	1	1 + 4
Energy range [GeV]	3–9	3–75
Reference	[7]	[8]

$d_{\text{SCI}} = 2.5 \text{ mm}$   $e/h = 1$  predicted for  $d_{\text{DU}} = 3.2 \text{ mm}$  and  $d_{\text{Pb}} = 10.0 \text{ mm}$ . This difference in  $d_{\text{ABS}}$  is due to the reduced production ( $\sim 2/3$ ) of slow primary neutrons in lead compared to uranium.

Table 2 and 3 give an overview of the different hadron calorimeter configurations studied by members

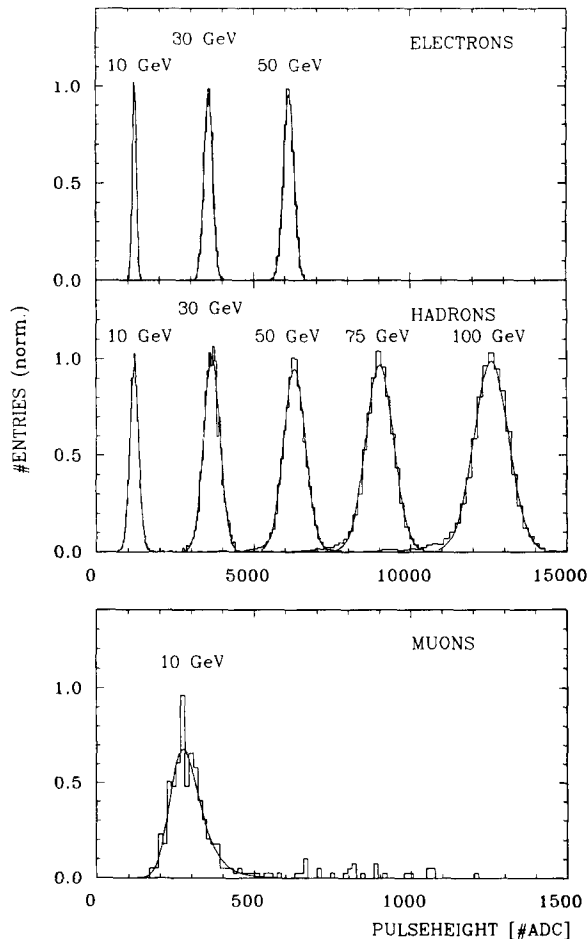


Fig. 3. Response of the test setup T60B for: a) Electrons. b) Hadrons. c) Muons.

of the ZEUS collaboration, as well as the references for a more detailed description.

For the relative calibration of the individual photomultipliers the photocurrent from the uranium radioactivity has been used for the uranium calorimeters. This calibration has been cross-checked using electrons, muons and  $\gamma$ -sources. The calibration of the lead calorimeters has been done with electrons, muons and  $\gamma$ -sources.

As an illustration of the performance of these calorimeters, fig. 3 shows the pulse height distribution

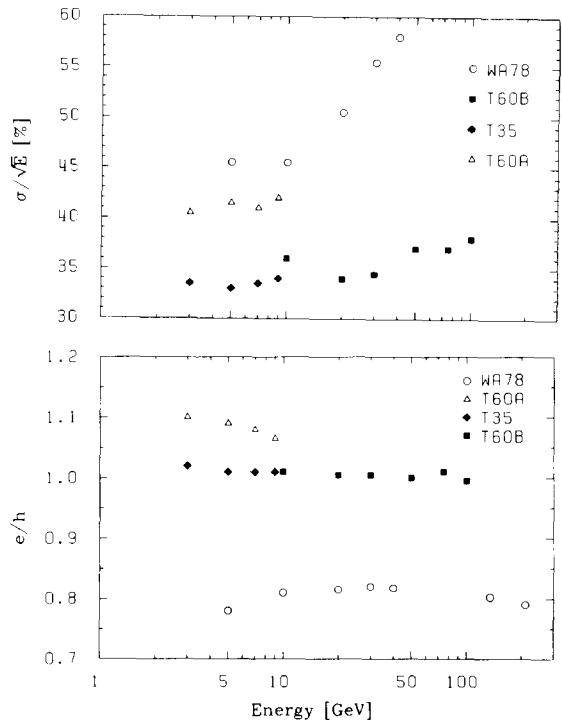


Fig. 4. Response of the uranium scintillator test calorimeters as function of energy. The data are corrected for transverse leakage and longitudinal readout uniformity. a) Standard deviation of the hadronic energy distribution  $\sigma_h/\sqrt{E_h}$ . b) Ratio of mean electron to hadron response.

for electrons and hadrons of different energies and muons of 10 GeV for the experiment T60B. The distributions for hadrons and electrons are well described by Gaussian functions for several standard deviations around the most probable value. At higher energies, deviations from Gaussian distributions are observed for lower pulse heights. They are ascribed to longitudinal energy leakage, and can be removed by eliminating events which have energy deposited in backing calorimeters which follow some of the test calorimeters. Mean values and standard deviations are obtained by fitting Gaussian functions in the region  $\pm 3$  standard deviations around the mean value.

Fig. 4a shows the energy resolution  $\sigma_h/\sqrt{E_h}$ , and fig. 4b the ratio of electron to hadron response  $e/h$  for the uranium scintillator calorimeters. Fig. 5 shows a comparison of the measured  $e/h$  ratio at 10 GeV with the prediction by Brückmann et al. [2]. We should notice that in particular the  $e/h$  ratios are very difficult to measure, as they critically depend on the uniformity of response achieved for the readout. For the data shown, an attempt has been made to correct for these effects to the best of the author's knowledge. For the data of ref. [6], the leakage correction as estimated in the publication has been used.

We note that T35 has achieved an energy resolution of  $\sim 34\%/\sqrt{E}$  in the range of 3–9 GeV and T60B a similar resolution at low energies, worsening to about  $38\%/\sqrt{E}$  at 100 GeV. These two calorimeters have a ratio of  $d_{ABS}/d_{SCI} \cong 1.2$  and both have  $e/h$  compatible with 1. The other two tests T60A and WA78/HERA have significantly different  $d_{ABS}/d_{SCI}$  ratios. Their  $e/h$  ratios are significantly different from one and the energy resolutions are significantly worse already at beam energies below 10 GeV and even more at higher energies. The data confirm the prediction that the best energy resolution, and the scaling of the resolution at  $1/\sqrt{E}$ , is achieved only for  $e/h \sim 1$ .

Fig. 6a and 6b show the energy resolutions  $\sigma_h/\sqrt{E_h}$

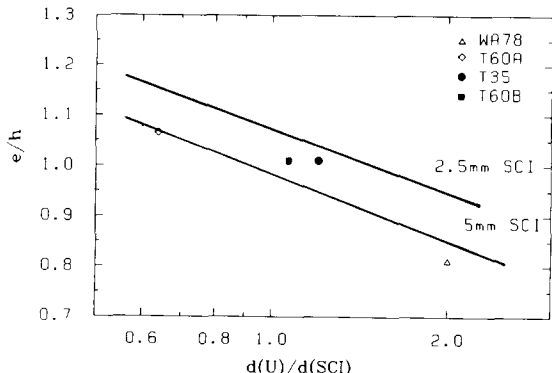


Fig. 5. Comparison of the measured electron to hadron ratio at 10 GeV to the predictions of H. Brückmann et al. [2].

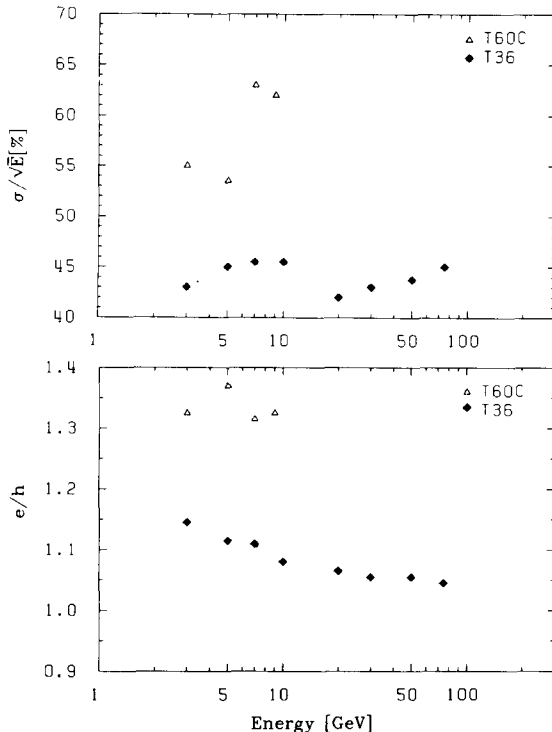


Fig. 6. Response of the lead scintillator test calorimeter as function of energy. a) Standard deviation of the hadronic energy distribution  $\sigma_h/\sqrt{E_h}$ . b) Ratio of mean electron to hadron response, corrected for transverse energy leakage.

and  $e/h$  ratios for the two lead tests. The data are corrected for nonuniformities and leakage. The response of the T36 calorimeter to electrons and hadrons of different energies and to muons at 10 GeV is shown in fig. 7.

As for the uranium calorimeters, the response can be well described by Gaussian functions, except for a low energy tail, which is ascribed to leakage, and which can be removed by cuts. For details we refer to the original paper [7,8]. Qualitatively the results are like those for the uranium calorimeters. The energy resolution improves with  $e/h$  approaching 1. For an absorber to detector ratio  $d_{Pb}/d_{SCI}$  of about 4, an  $e/h$ -ratio of 1.05 with an estimated uncertainty of 0.05, and an energy resolution of  $\sigma_h/\sqrt{E_h} \sim 44\%$  is achieved. For the readout method chosen (plates of scintillator readout via wave length shifter) the chosen 2.5 mm thickness of scintillator represents a practical lower limit. Thus 10 mm Pb plates had to be chosen, which resulted in the poor electromagnetic energy resolution of  $\sigma_e/\sqrt{E_e} \sim 24\%$  and possibly in a significant contribution of sampling fluctuations to the hadronic energy resolution.

On the basis of these measurements, detailed Monte Carlo studies and the successful use of the natural radioactivity of uranium for calibration, the ZEUS col-

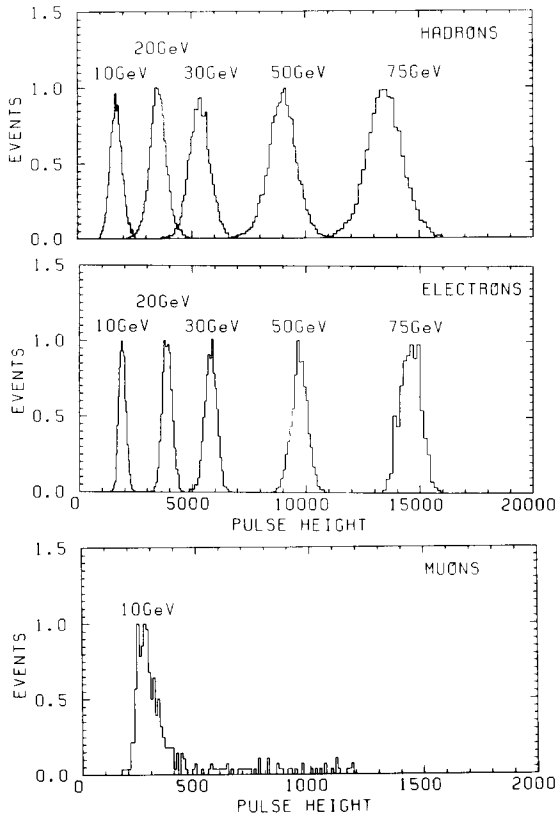


Fig. 7. Response of the lead scintillator calorimeter T36 for: a) Hadrons. b) Electrons. c) Muons.

laboration has chosen a sampling structure of 3.3 mm depleted uranium, clad with thin (0.2 to 0.4 mm) steel sheets, and 2.6 mm of plastic scintillator SCSN-38 for the high resolution calorimeter.

#### 4. Influence of readout uniformity

The ZEUS collaboration has set as its goal for the performance of the calorimeter an electromagnetic energy resolution of  $15\%/\sqrt{E}$  with a constant term of about 2%, and a hadronic energy resolution of  $35\%/\sqrt{E}$  with a constant term below 2%. This can only be achieved via excellent uniformity of response, low noise and precise cell-to-cell calibration.

Detailed experimental and Monte Carlo studies of the influence of nonuniformity of readout and inhomogeneities of the calorimeter on  $e/h$  ratios and energy resolutions have been performed. Here we present measurements which convince us that the effect of the wavelength shifter gap between adjacent modules does not result in an unacceptable calorimeter performance. First we note that in the ZEUS calorimeter there are no gaps which directly project to the interaction point. As

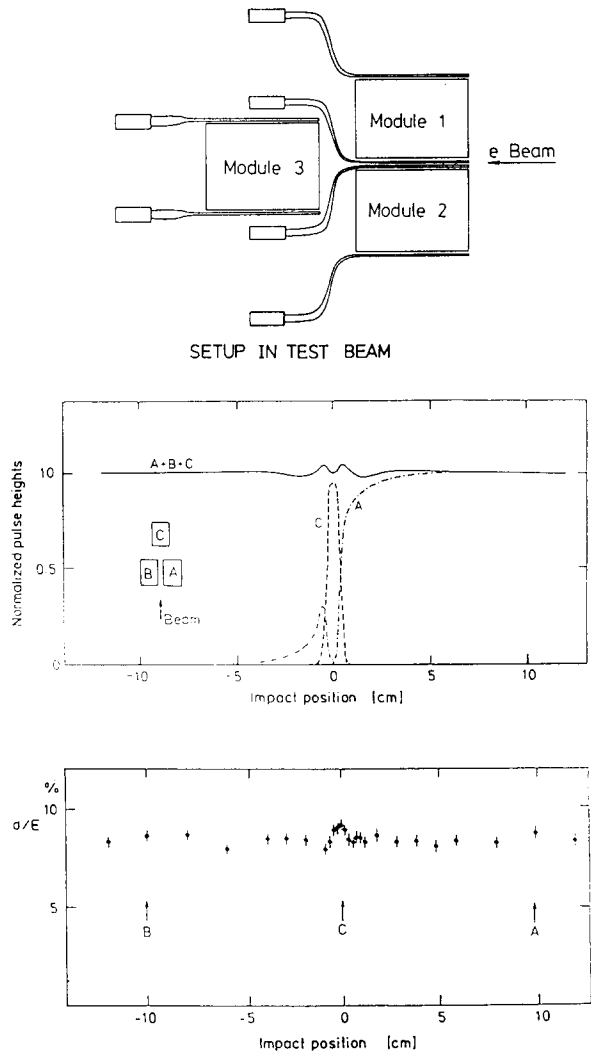


Fig. 8. Three calorimeter test to measure the influence of the wavelength shifter gap on the response of a lead scintillator calorimeter. a) Experimental setup. b) Mean energy  $\langle E \rangle$  as function of impact point of the beam for 3 GeV electrons. c) Standard deviation of the energy distribution as function of the impact point of the beam for 3 GeV electrons.

a result all particles will sooner or later traverse absorption material. By choosing the proper response of the wave shifting material to charged particles, via doping with UV-absorbant, the ratio of light yield to energy loss in the wave shifter matches approximately the corresponding ratio in the uranium scintillator calorimeter. In this case the wavelength shifter gaps do not worsen the energy resolution, but only change the longitudinal shower distributions. This has been demonstrated by a setup of 3 electromagnetic calorimeters as shown in fig. 8a [9]. The sampling structure of the calorimeters was 6 mm of lead and 5 mm of SCSN-38

plastic scintillator. Fig. 8b shows the mean response and fig. 8c the standard deviation of the energy response for 3 GeV electrons, when scanning the beam over the gap between the calorimeter. The maximum change in response is  $\pm 2\%$  in a small region around the gap, and there is hardly any change in the energy resolution. In particular deviations from the Gaussian response functions are absent. Using the data as input to estimate the energy resolution for hadron jets indicates negligible effects. These measurements will be repeated with a calorimeter of the final geometry and sampling structure.

**5. Radiation stability of plastic scintillator and wavelength shifter**

Radiation damage of the optical components is one of the major worries if one uses scintillator to read out a calorimeter at a high luminosity storage ring. There are many reports of performance degrading with time due to radiation damage or scintillator aging.

The systematic investigation of radiation damage is difficult due to the many parameters on which it depends, such as:

- production technology of the material,
- purity of the base materials,
- type of ionising radiation,
- radiation dose and dose rate,
- environmental conditions (gas, temperature, humidity etc).

Members of the ZEUS collaboration [10] have started systematic studies for the materials to be used in the ZEUS calorimeter: SCSN-38 for plastic scintillator, plexiglass doped with K-27 or Y7 for wavelength shifting, and plexiglass doped with UV-absorbant as light guide. Irradiations have been done with 25 MeV protons,  $\gamma$ 's from  $^{60}\text{Co}$  and low energy electrons for different doses and dose rates, in air, nitrogen and argon. The investigations include light transmission measurements as function of wavelength using a spectral photometer for thin samples (typically few mm). For longer samples light yield and light transmission over longer distances are measured by scanning the scintillator with light from a pulsed UV lamp appropriately filtered, or electrons from radioactive sources. The pulse heights of individual events are measured and accuracies below  $\sim 1\%$  are achieved.

Fig. 9 shows a typical result. A SCSN-38 bar of dimensions  $0.3 \times 2 \times 26$  cm has been irradiated with protons of 25 MeV to a total dose of 1 kGy, leaving 3 narrow regions at the beginning, middle and end of the strip nonirradiated. The atmosphere was either air or nitrogen. For the measurement one end of the scintillator was covered with black velvet, the other edge coupled via a wavelength shifter to a photomultiplier. The

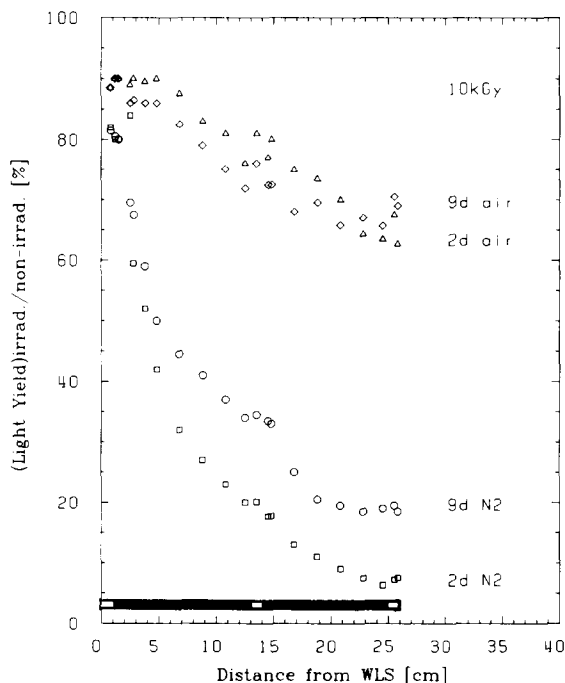


Fig. 9. Radiation damage studies for 2.5 mm thick plastic scintillator SCSN-38. Shown in the pattern of irradiation and the ratio of pulse height measured by excitation with light from a xenon lamp after and before irradiation. Data presented for irradiation with 10 kGy of 25 MeV protons for material stored in air and nitrogen. Measurements have been done 2 days and 9 days after irradiation.

light was excited via a xenon flashlamp filtered to a wavelength of  $\sim 340$  nm. Fig. 9 shows the ratios of light yields after irradiation to before irradiation as function of the distance from the wavelength shifter. The measurements were done 2 days and 9 days after irradiation and storage in the indicated gases. A comparison of light yield ratios in the nonirradiated region in the center to the close-by irradiated regions measures the change in light yield. The dependence of the decrease of the ratio on the distance from the wavelength shifter measures the attenuation of the light. In both air and nitrogen, we find a small (few percent) decrease of the produced light, whereas there is a significant increase in light attenuation in particular for the exposures in nitrogen.

Fig. 10 shows for irradiation with 1 kGy and 10 kGy the change in light yield, as defined above, and the change in light attenuation, defined as:

$$\frac{\text{Light}(x = 18.8 \text{ cm})/\text{Light}(x = 2.8 \text{ cm})\Big|_{\text{irradiated}}}{\text{Light}(x = 18.8 \text{ cm})/\text{Light}(x = 2.8 \text{ cm})\Big|_{\text{nonirradiated}}}$$

as a function of the days between irradiation and measurement. It can be concluded that at 10 kGy there is



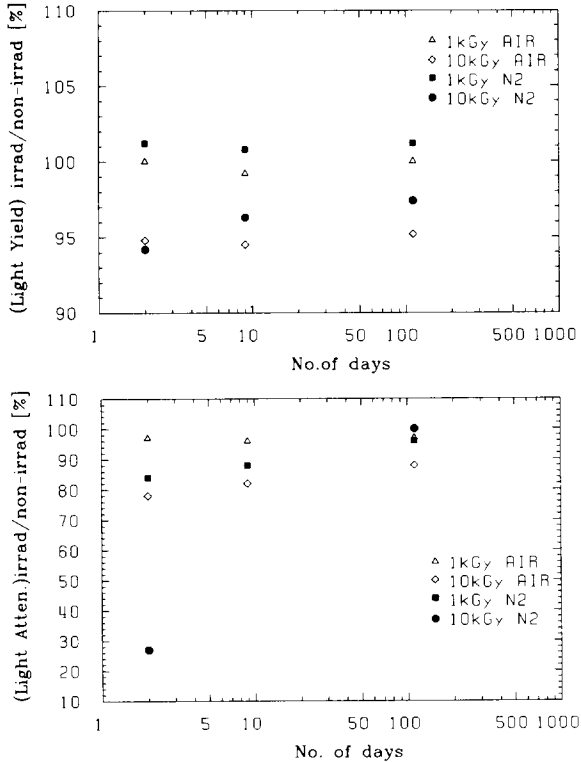


Fig. 10. Measurement of light yield and light attenuation for 2.5 mm thick scintillator SCSN-38 for 1 kGy and 10 kGy irradiation with 25 MeV protons. Measurements are done for material stored in air or nitrogen and have been performed 2, 9 and 111 days after the irradiation. For the exact definition of the quantities measured see text.

about a 5% reduction in light yield, possibly slowly recovering with a time constant of more than 100 days, quite independent of the gas. The light transmission is strongly reduced, in particular in nitrogen; it however recovers with time constants of the order of hundred days. These observations have been confirmed by measurements with low energy electrons and the spectral photometer. We should also note that in the region of highest radiation dose in the ZEUS experiment, the maximum scintillator dimensions are  $\sim 20$  cm.

For a wavelength shifter made from plexiglas with 120 mg/l K-27 doping, irradiated to 10 kGy via 25 MeV protons, the measurements are shown in fig. 11. There is a strong radiation damage in air and in nitrogen. Whereas the damage completely recovers in air after about 100 days, it is permanent or even worsening in nitrogen. For the ZEUS calorimeter the maximum length of wavelength shifters is about 70 cm.

The maximum radiation dose to which the optical components of the ZEUS calorimeter will be exposed have been estimated to be:

- 6 Gy per year from uranium with 0.2 mm cladding,

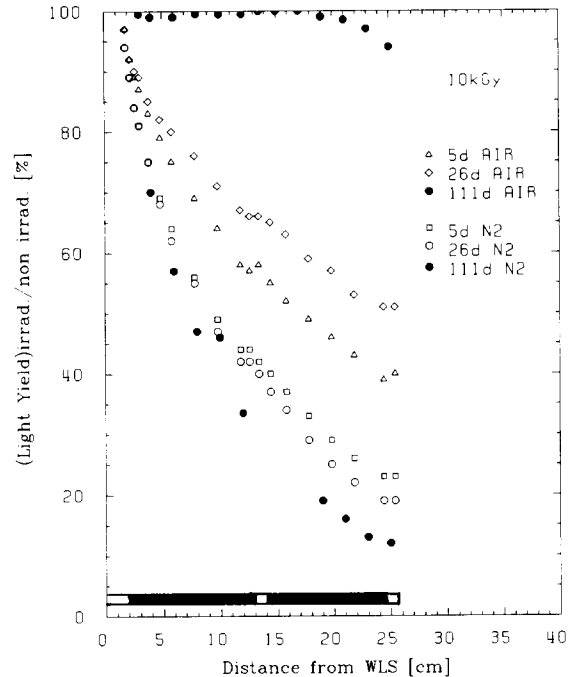


Fig. 11. Radiation damage studies for 2 mm thick plexiglass doped with 120 mg/l K-27. Shown is the pattern of irradiation and the ratio of pulsed height measured by excitation with light from an SCSN-38 scintillator after and before irradiation. Data are shown for irradiation with 10 kGy of 25 MeV protons for materials stored in air and nitrogen. Measurements have been done 5, 26 and 111 days after irradiation.

- 2.2 Gy per year from uranium with 0.4 mm cladding,
- 300 Gy per year from HERA, close to the beams,
- 10 Gy per year from HERA, about 1.2 m away from the beam.

The studies of radiation damage are continuing, but presently we think that with the chosen materials for scintillator, wavelength shifters and light guides and special care in particular at the early stages of HERA (e.g. move front and rear calorimeters 40 cm away from the beam during injection) we shall be able to cope with the problems of radiation damage.

## 6. Conclusions

This paper gives a short review of some of the research and development work done by the ZEUS collaboration towards a high resolution calorimeter for the HERA storage rings. The most important results are:

- the technique of achieving equal response for electrons and hadrons and an energy resolution of  $\sigma/E \sim 35\%\sqrt{E}$  for hadrons using uranium as absorber and plastic scintillator as pioneered by Fabjan and

Willis [11] has been confirmed. The measurements quantitatively follow the recent predictions. In particular they confirm the important role of the proper detection of the signal from low energy neutrons,

- it has been shown for the first time that compensation can also be achieved using lead and scintillator,
- various problems related to nonuniformities in a calorimeter using scintillator and wavelength shifter have been studied and partially solved,
- studies of radiation damage indicate that by proper choice of materials and gases this problem can be overcome for the Zeus calorimeter at HERA.

During 1987 ZEUS will build prototype calorimeters with the final geometries to confirm the optimisation which has lead to the present design. The start of the construction of the final calorimeter modules is planned for the first half of 1988.

#### Acknowledgement

The author would like to thank his many colleagues working on the calorimeter of the ZEUS detector for their collaboration, and the permission to present some of their work. The measurement would not have been possible without the excellent technical help from our home institutes, in particular from NIKHEF-H at Amsterdam, DESY at Hamburg, and the Universities of Hamburg and Rome. Most of the beam test have been performed at CERN, and we should like to thank CERN for the hospitality and the technical support.

#### References

- [1] The ZEUS detector, Technical Proposal, DESY (March 1986), and Status Report 1987, DESY (Nov. 1987).
- [2] H. Brückmann, U. Behrens and B. Anders, Hadron Sampling Calorimetry – A Puzzle of Physics (Dec. 1986) DESY 86-155.
- [3] R. Wigmans, On the Energy Resolution of Uranium and other Hadron Calorimeters (Sept 1986) CERN/EF 86-18.
- [4] M.G. Catanesi et al., Hadron-, Electron- and Muon-Response of a Uranium-Scintillator Calorimeter, DESY 87-027 (April 1987).
- [5] J. Krüger, Shower Development in a Uranium-Scintillator Calorimeter and the Requirements for the Hadron Calorimeter of the ZEUS detector, ZEUS Note 86-019 (May 1986).
- [6] B. Anders et al., Performance of a Uranium-Scintillator Calorimeter, DESY 86-105 (September 1986).
- [7] J. Engelen and H. Tiecke, Performance of a Hadron Test Calorimeter for the ZEUS Experiment, NIKHEF-H/86-18.
- [8] E. Bernardi et al., Performance of a Compensating Lead-Scintillator Hadronic Calorimeter, DESY 87-041 (May 1987).
- [9] E. Bernardi, R. Klanner, U. Kötz and G. Levman, Uniformity Test on an Electromagnetic Calorimeter with Wavelength Shifter Readout, ZEUS Note 86-020 (June 86); R. Klanner, B. Löhr, E. Ros and S. Weissenrieder, Light Yield and Uniformity of an Electromagnetic Calorimeter with Wavelength Shifter Readout, ZEUS Note 86-042 (October 1986).
- [10] The author should like to thank U. Holm and K. Wick from the University of Hamburg for detailed discussions on their investigations on radiation damage. The data presented have been measured by U. Holm from the University of Hamburg, 1st Inst. for Experimental Physics.
- [11] C.W. Fabjan et al., Nucl. Instr. and Meth. 141 (1977) 61; T. Akesson et al., Nucl. Instr. and Meth. A241 (1985) 17.